Supercontinuum Generation in Silica Fibers by Amplified Nanosecond Laser Diode Pulses

Chenan Xia, Malay Kumar, Ming-Yuan Cheng, Ojas P. Kulkarni, Mohammed N. Islam, *Fellow, IEEE*, Almantas Galvanauskas, Fred L. Terry, Jr., *Senior Member, IEEE*, Mike J. Freeman, Daniel A. Nolan, *Member, IEEE*, and William A. Wood

***Abstract*—Supercontinuum (SC) with a continuous spectrum from ~ 0.8–3 μm is generated in a standard single-mode fiber followed by high-nonlinearity fiber. The SC is pumped by 2-ns laser diode (LD) pulses amplified in a multistage fiber amplifier, and the two octave spanning continuum is achieved by optimizing a two-stage process that separates pulse breakup and soliton formation from spectral broadening. We also demonstrate scalability of the average power in the continuum from 27 mW to 5.3 W by increasing the pulse repetition rate from 5 kHz to 1 MHz, while maintaining comparable peak power. We attribute the generated SC spectrum to the ensemble average of multiple solitons and the superposition of their corresponding spectra. The hypothesis is confirmed through simulation results obtained by solving the generalized nonlinear Schrödinger equation (NLSE). Similar SC spectra can also be obtained by using both femtosecond and nanosecond pump pulses. Furthermore, by tailoring the input pulse shape, we propose and simulate the generation of the entire SC spectrum in one single soliton under quasi-continuous-wave (CW) pulse pumping scheme.**

***Index Terms*—Midinfrared, modulation instability (MI), soliton, supercontinuum (SC).**

I. Introduction

BROADBAND supercontinuum (SC) generation in fused silica fibers has been reported using a variety of pump sources in recent years [1]. Two approaches of generating continuum are widely used—pumping a short length of highly nonlinear (HiNL) fiber with femtosecond or picosecond pulses [2] or using continuous wave (CW)/quasi-CW sources to pump long lengths ($>$100 m) of fiber [3]. The broadening mechanism in the former can be attributed primarily to self-phase modulation (SPM), while in the latter, spectral broadening is achieved due to the combined effects of parametric four-wave mixing and stimulated Raman scattering (SRS) [4]–[6]. For example, a mode-locked femtosecond erbium fiber laser was used to generate 400 mW of SC output from 0.8–2.7 μm in just 12 cm of HiNL fiber [2]. In contrast, Abeeluck *et al*. demonstrated a continuum extending beyond 1.75 μm with $\sim$5-W average power in 500 m of HiNL fiber pumped by a CW Raman fiber laser [3]. Recently, SC generation from ~ 0.8 to 1.7 μm in a dispersion-shifted fiber has also been demonstrated by using amplified laser diode (LD) pulses with 30-ps pulse width [7].

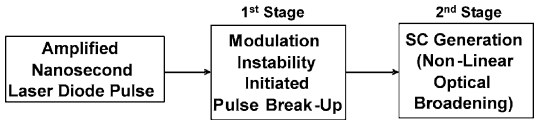

Fig. 1. Two-step SC generation process: pulse breakup in single-mode fiber followed by spectral broadening in HiNL fiber.

In this paper, we demonstrate a fused silica-fiber-based SC light source extending to ~ 3 μm with time-averaged power scaled up to 5.3 W. By using modulation instability (MI) in the fiber [6], the pump requirements are simplified, and the broad spectrum is obtained with nanosecond pulses and a few meters of fused silica fiber. The pump consists of 2-ns LD pulses, which are amplified to $\sim$4-kW peak power in a multistage fiber amplifier. The pulses are launched into 2–3 m of standard single-mode fiber to initiate MI-induced pulse breakup, and then spectrally broadened in $<$1-m length of HiNL fiber to obtain a continuum ranging from ~ 0.8–3 μm. The average power of the SC is scalable from $\sim 27\,\mathrm{mW}$ to $5.3\,\mathrm{W}$ by varying the pulse repetition rate and using a cladding-pumped fiber amplifier. In addition, simulations have been carried out by solving the generalized nonlinear Schrödinger equation (NLSE) and agree well with the experiments. The potential applications of the demonstrated high-power wideband light source include spectroscopy, chemical sensing, and optical coherence tomography [8].

We generate a broad continuum by implementing the SC generation as a two-step process (Fig. 1). In the first stage, 1.55-$\mu\mathrm{m}$ LD pulses are launched into a single-mode fiber, where the interaction between nonlinearity and anomalous dispersion breaks the quasi-CW input into a train of solitons through MI [5]–[7], [9], [10] and significantly increases the peak power. Thus, while many SC generation experiments use mode-locked femtosecond lasers to achieve high peak powers, MI enables the use of long pulses from compact sources such as LDs and facilitates the SC generation. The generated solitons will then undergo frequency down-shift through soliton self-frequency shifting (SSFS) [5], [11]. In the second-stage HiNL fiber, the SC spectrum is further broadened primarily through the SPM effects of the ultrashort solitons [10], [12]. By choosing the HiNL fiber with a zero-dispersion wavelength close to the pump

Manuscript received February 16, 2007; revised April 2, 2007. This work was supported in part by the Army Research Office, in part by Defense Advanced Research Projects Agency (DARPA), and in part by Omni Sciences, Inc.

C. Xia, M. Kumar, M.-Y. Cheng, O. P. Kulkarni, A. Galvanauskas, and F. L. Terry, Jr., are with the Department of Electrical Engineering and Computer Science, University of Michigan, Ann Arbor, MI 48109 USA (e-mail: caxia@umich.edu).

M. N. Islam is with the Department of Electrical Engineering and Computer Science, University of Michigan, Ann Arbor, MI 48109 USA, and also with Omni Sciences, Inc., Ann Arbor, MI 48105 USA (e-mail: mni@eecs.umich.edu).

M. J. Freeman is with Omni Sciences, Inc., Ann Arbor, MI 48105, USA.

D. A. Nolan and W. A. Wood are with the Research, Development and Engineering Division, Corning, Inc., Corning, NY 14831 USA.

Digital Object Identifier 10.1109/JSTQE.2007.897414

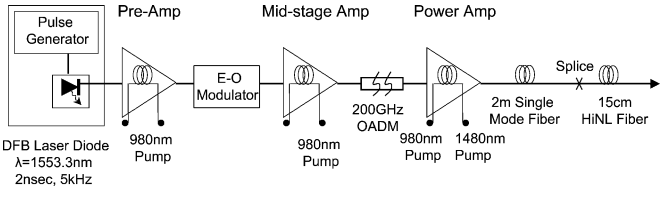

Fig. 2. Low average power experimental setup: LD pulses amplified by single-mode EDFAs.

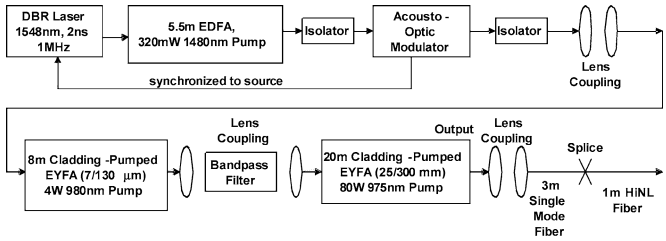

Fig. 3. High average power experimental setup: LD pulses amplified by cladding-pumped erbium/ytterbium codoped fiber amplifiers.

wavelength, the SC generation also benefits from parametric four-wave mixing effects due to the reduced dispersion of the nonlinear fiber [6]. The ensemble average of these solitons, which spread over the entire nanosecond-wide pulse, gives rise to the broad, smooth SC spectrum [5], [11], [13]. Simulations show that similar spectra can be generated by using both femtosecond and nanosecond pump lasers. The nanosecond LD pumping also simplifies the scaling up of the time-averaged power. Since the nonlinear phenomena responsible for SC generation are related to the peak power of the pump pulses, the average power in the continuum can be increased simply by increasing the pulse duty cycle while keeping the peak power approximately constant. To further concentrate the majority of the energy of the generated SC, we simulate and propose to generate the entire SC spectrum in a single soliton pulse by tailoring the temporal profile of the amplified LD pulses.

This paper is organized as follows. In Section II, we describe the experimental setup and illustrate the experimental results. In Section III, we simulate the SC generation by solving the generalized NLSE. The generated SC spectrum by amplified nanosecond pulses is composed of the ensemble average of the multisolitons. In Section IV, we propose a novel method to generate the entire SC spectrum in a single soliton pulse by tailoring the shape of the amplified LD pulse. Finally, we summarize the experimental and simulation results in Section V.

II. Experimental Setup and Results

SC generation experiments are performed at two different repetition rates—5 kHz and 1 MHz. The experimental setup for the low average power system (5 kHz) is illustrated in Fig. 2. A distributed feedback (DFB) LD at 1553 nm is driven by a pulse generator to provide 2-ns signal pulses at a 5-kHz repetition rate, corresponding to a duty cycle of 100 000:1 [10]. The pulses are amplified to ~ 4.7-kW peak power in three stages of single-mode erbium-doped fiber amplifiers (EDFA). We use an electrooptic modulator to suppress the in-band amplified spontaneous emission (ASE), while a 200-GHz optical add/drop multiplexer (OADM) removes the out-of-band ASE. The setup is made entirely of telecommunication components and fusion spliced together with no free-space elements. To generate a wide SC, the output of the power-amp is spliced to the first-stage single-mode fiber to breakup the amplified 2-ns pulses into ultrashort soliton pulses. The single-mode fiber output is then spliced to the second-stage HiNL fiber to achieve the desired spectral broadening. The HiNL fiber used in the experiment has a zero-dispersion wavelength of 1544 nm and a dispersion slope of $0.044\,\mathrm{ps}/(\mathrm{km}\cdot\mathrm{nm}^2)$ at the pump wavelength. The HiNL fiber is extra water-dried to minimize the water composition in the fiber. With an effective mode area of $\sim 10\ \mu\mathrm{m}^2$, the HiNL fiber has a nonlinearity coefficient of $\sim 9.6\ \mathrm{W}^{-1}\mathrm{km}^{-1}$. An optical spectrum analyzer is used to measure the lower end of the SC spectrum (800–1750 nm), while the long-wavelength spectrum is acquired by a nitrogen-purged grating spectrometer. A low-noise TE-cooled InAs detector connected to a lock-in amplifier is used to reliably measure the long-wavelength spectrum with more than 40 dB of dynamic range.

To scale up the average power in the SC, the pulse repetition rate of the pump is increased from 5 kHz to 1 MHz, while keeping the peak pump power almost constant. The high-power system (Fig. 3) at 1 MHz (duty cycle of 500:1) has a similar experimental setup as does the 5-kHz system, with a distributed Bragg reflector (DBR) LD producing 2-ns pulses that are amplified through three stages of fiber amplifiers [14]. To suppress the stimulated Brillouin scattering, the signal spectrum of the laser is broadened to ~ 1-nm bandwidth by chirping the phase segment of the diode. The system consists of three main amplification stages: a standard single-mode core preamplifier, a 7-μm core double-clad fiber amplifier, and a 25-μm core double-clad fiber amplifier. The preamplifier stage is a 5.5-m-long EDFA pumped by a 320-mW 1480-nm pump diode. The second stage is an 8-m-long single-mode erbium/ytterbium codoped fiber amplifier (EYFA), which has a 7-μm numerical aperture (NA) $= 0.17$ core and a 130-$\mu\mathrm{m}\ \mathrm{NA} = 0.46$ inner pump cladding. The ASE of the first- and second-stage fiber amplifiers is suppressed by using an acoustooptic modulator and a bandpass filter. The last stage is a 20-m-long large-mode-area EYFA, which has a 25-$\mu\mathrm{m}\ \mathrm{NA} = 0.1$ core and a 300-$\mu\mathrm{m}\ NA = 0.46$ cladding. Large-mode-area fiber is used to avoid nonlinear effect in the fiber core, and single-mode output can be achieved by properly matching the mode of the input beam with the fundamental mode of the gain fiber. The power-amp of this system provides a free-space output with 8.8-kW peak (17.6 W average) power with ~ 80-W pump power, of which 3.8 kW (7.6 W) is coupled into the first-stage single-mode fiber.

A broad continuum extending from ~ 0.8 to $\sim 3\ \mu$m is obtained with the 5-kHz system for 2-m single-mode fiber followed by 15-cm length of HiNL fiber. The resulting spectrum after the single-mode fiber for 4.7-kW peak (47 mW average) input power is shown in Fig. 4. The red-shifted spectrum after the single-mode fiber extends from 1.4–2.5 μm and is primarily attributed to the SSFS effect. After the HiNL fiber stage, there is

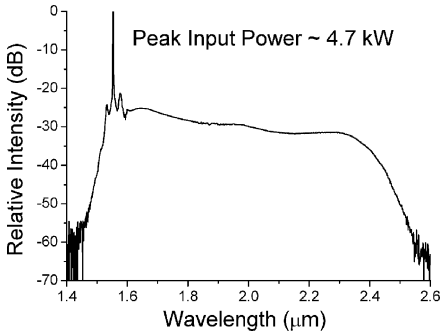

Fig. 4. Spectrum after 2-m single-mode fiber for 4.7-kW peak input power in the low-power setup.

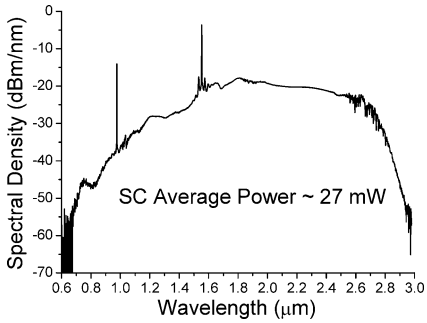

Fig. 5. 27-mW average power SC spectrum after 2-m single-mode fiber and 15-cm HiNL fiber in the low-power setup.

SPM-induced spectral broadening, which further pushes out the spectrum to ~ 3 μm on the long-wavelength side and ~ 800 nm on the short-wavelength side. The resulting SC is shown in Fig. 5. Both spectra have been calibrated by including the wavelength response of the grating and InAs detector. We measure the average power in the continuum to be ~ 27 mW, thus, achieving a $\sim 60\%$ power conversion efficiency from pump to continuum. The spectral peak around 1550 nm is due to the LD pump while the peak at 980 nm is due to the undepleted counterpropagating pump of the power-amp. We also observe multiple absorption lines between 2.5–2.8 μm and attribute these to the water absorption in the spectrometer.

To confirm that the SC is initiated by MI, we measure the temporal autocorrelation and spectrum after the first-stage single-mode fiber. The results after propagation through 3-m single-mode fiber at 1-kW peak input power are shown in Fig. 6. The autocorrelation [Fig. 6(a)] shows the formation of short pulses with pulse envelop of ~ 500 fs, and the background level is due to the lower intensity pulse wings. The spectrum shows two sets of characteristic MI sidebands, with the first-order sidebands separated by ~ 18 nm from the pump at 1553 nm. The frequency shift of the first-order MI gain peaks from the pump is given by $\Delta\omega = (2\gamma P_0/|\beta_2|)^{1/2}$, where γ is the nonlinearity coefficient, P_0 is the peak power of the pump, and β_2 is the group velocity dispersion parameter of the fiber at the pump wavelength. For single-mode fiber pumped by 1-kW pulses at 1.55 μm, $\gamma = 1.6\,\mathrm{W^{-1}km^{-1}}$, $\beta_2 = -18\mathrm{ps}^2/\mathrm{km}$, and the calculated frequency shift $\Delta\nu = 2.12$ THz. The corresponding wavelength separation is ~ 17 nm, which is close to the

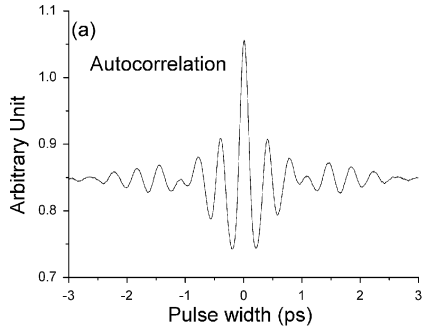

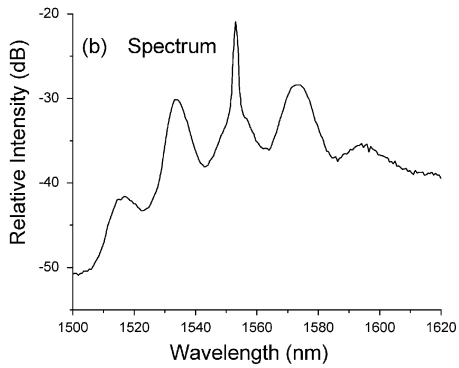

Fig. 6. MI-induced pulse breakup in single-mode fiber. (a) Autocorrelation. (b) Spectrum. The results are shown for 3 m of single-mode fiber at 1-kW peak input power.

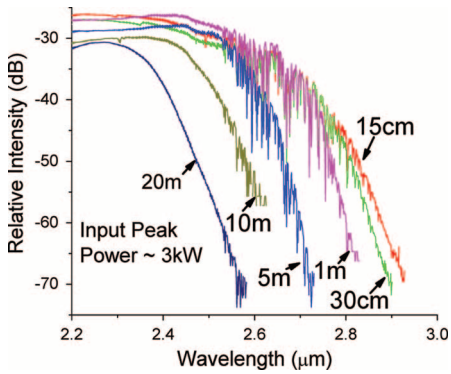

Fig. 7. Optimization of HiNL fiber length to achieve the longest SC edge: spectrum after 2-m single-mode fiber followed by varying lengths of HiNL fiber.

experimentally observed value in Fig. 6(b). We observe that the 1530-nm MI gain peak coincides with the ASE peak from the EDFA, and thus, the pulse breakup process is seeded by the ASE.

To optimize the second stage, we studied the spectral evolution of the SC as a function of HiNL fiber length for a fixed length of single-mode fiber. Fig. 7 shows the long-wavelength spectrum for a 2-m length of single-mode fiber followed by varying lengths of HiNL fiber, with each plot being on the same scale relative to the others. As the HiNL fiber length is cut back from 20 m down to 15 cm, the long-wavelength edge of the SC increases from 2.6 μm to ~ 3 μm along with an increase in the overall spectral density. These results indicate that the

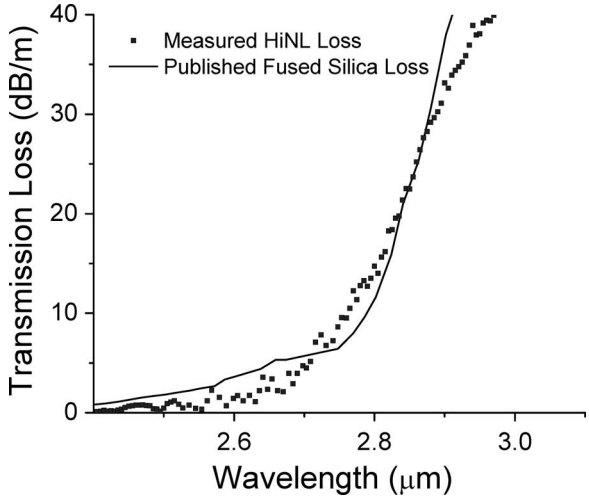

Fig. 8. Transmission loss in HiNL fiber. Dotted curve shows experimental results while solid curve shows previously published data.

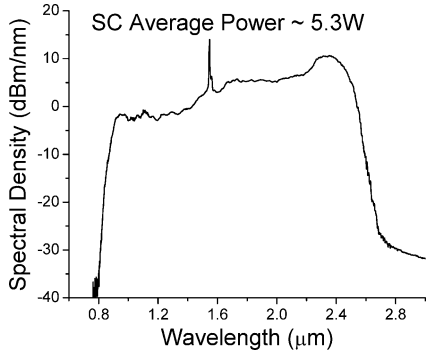

Fig. 9. 5.3-W average power SC. Spectrum after 3 m of single-mode fiber and 1-m HiNL fiber for ~3.8-kW peak input power.

nonlinear processes responsible for the wide spectrum generation occur within the first few centimeters of the HiNL fiber, and propagation through longer lengths merely attenuates the spectrum due to the high loss associated with the silica glass absorption around 3 μm. Thus, obtaining the broadest spectrum requires the shortest fiber length where nonlinearity dominates over loss.

Furthermore, we measure the transmission loss of the HiNL fiber as a function of wavelength. The loss curve is shown in Fig. 8. It is found that the loss increases rapidly beyond 2.7 μm and is as high as 40 dB/m at ~2.9–3 μm. The loss can be possibly attributed to the water absorption, bend-induced loss, and intrinsic silica glass absorption. By comparing the SC from non-dried fibers with that of dried fibers of 3–5-m lengths, the edge only extends $\sim 100\,\mathrm{nm}$ and still does not go beyond 2.8 μm, which suggests that water absorption plays a role but is not the dominant limitation. Fibers with different core sizes and a similar index profile also give comparable edges to the SC spectrum, which downplays the significance of the bend-induced loss. Finally, the measured loss curve is in good agreement with previously published results [15], and thus, shows that the intrinsic silica loss due to vibrational absorption limits the long-wavelength edge of the SC.

The time-averaged power in the continuum is scaled up to 5.3W by increasing the repetition rate of the system from 5 kHz to 1 MHz and using the cladding-pumped fiber amplifiers. The spectrum after 3-m single-mode fiber followed by 1-m HiNL fiber for 3.8-kW peak (7.6 W average) input power is shown in Fig. 9 and extends from 0.8–2.8 μm. For the 5-kHz system, the power in the continuum is $\sim 27\,\mathrm{mW}$, while for the 1-MHz system, it is $\sim 5.3\,\mathrm{W}$. Thus, the power is scaled up by a factor of ~ 195 and is consistent with the $200\times$ increase in the repetition rate.

The difference in the single-mode fiber lengths is attributed to the different fiber amplifiers used in the two systems. We notice that the broadest SC requires 3-m single-mode fiber at 1 MHz but only 2 m at 5 kHz. For the 5-kHz system, the pulse breakup is enhanced by the EDFA ASE, and the nonlinear effects start within the power-amp itself. But the large-mode-area EYFA in the 1-MHz system is designed for the minimal nonlinear broadening, and thus, longer lengths of single-mode fiber are required to achieve a similar pulse breakup. In addition, the high average power system has about 20% lower peak power (3.8 kW) compared to the low average power system (4.7 kW). Furthermore, the difference in spectral shape of the SC in Fig. 9 compared to Fig. 3 may be attributed to the lower peak power and longer HiNL fiber length in the 1 MHz system.

III. Simulations

To further investigate and understand the SC generation mechanism under different pump systems, we numerically solve the generalized NLSE. The complex envelope $A(z,\tau)$ of a pulse under the slowly varying approximation satisfies the generalized NLSE given by [6]

$$\frac{\partial A}{\partial z} = (\hat{D} + \hat{N})A$$

$$\hat{D} = -\frac{i}{2}\beta_2\frac{\partial^2 A}{\partial \tau^2} + \frac{1}{6}\beta_3\frac{\partial^3 A}{\partial \tau^3} + \frac{i}{24}\beta_4\frac{\partial^4 A}{\partial \tau^4} - \frac{\alpha}{2}$$

$$\hat{N} = i\gamma\left(1 + \frac{i}{\omega_0}\frac{\partial}{\partial t}\right)\int_{-\infty}^{+\infty}\left((1-f_R)\delta(t) + f_R h_R(t)\right] \times |A(z,t-t')|^2\,dt'$$

where the pulse moves along the z-direction in the retarded time frame $\tau = t - z/v_g$ with the center angular frequency of ω_0. The linear terms in the differential operator $\hat{D}$ account for the second- (β_2), third- (β_3), and fourth-order (β_4) dispersion as well as the loss (α) of the fiber. The terms in the operator $\hat{N}$ result from nonlinear interactions, which describe SPM, self-steepening, and SRS effects. In particular, the effective nonlinearity is defined as $\gamma = n_2\omega_0/cA_{\mathrm{eff}}$, where n_2 is the nonlinear refractive index and A_{eff} is the effective mode area of the fiber. In addition, $h_R(t)$ represents the Raman response function, and f_R is the fractional contribution of the Raman response to the nonlinear polarization.

The NLSE described previously has been solved by an adaptive split-step Fourier method with the initial pulse shape as the known boundary value [5], [16]. To reduce the computation

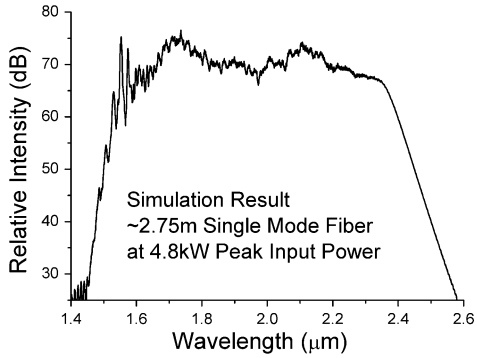

Fig. 10. Simulation result of low average power continuum after 2.5-m single-mode fiber at 4.8-kW peak power.

time, we assume a 100-ps super-Gaussian pulse at 1553 nm as the input to our simulator. Simulations with pulse widths ranging 30–200 ps have also been conducted and show the same results. Furthermore, the step size is determined and dynamically adjusted by the nonlinear gain in each section. Because of the large bandwidth of the SC compared to the Raman gain spectrum of the silica glass, approximation of the Raman gain as a linear function of frequency is not valid any more. Therefore, we take into account the actual Raman gain spectrum of the specific fiber in the simulator. For the single-mode fiber, the effective nonlinearity γ is $1.6\,\mathrm{W^{-1}km^{-1}}$ and Raman gain peak g_R is $6.4 \times 10^{-14}\mathrm{m/W}$ [6]. The HiNL fiber used in the experiment has a zero-dispersion wavelength at 1544 nm with the effective nonlinear coefficient assumed to be $9.6\,\mathrm{W^{-1}km^{-1}}$.

The simulation is performed in three distinct stages in the low average power setup. The first stage simulates the output after the amplifier, i.e., before the single-mode fiber, by including the nonlinearity in the gain fiber. Due to large peak powers developed in the last-stage amplifier and same core size of the gain fiber, we observe some spectral broadening at this stage itself, which is primarily attributed to the MI seeded by the 1530-nm ASE from the amplifier.

The output from the amplifier stage is then coupled into a 2.5-m length of single-mode fiber. The spectrum is red-shifted to $\sim 2.5\ \mu$m in the simulation, as shown in Fig. 10. In the corresponding time domain, we observe that the 100-ps super-Gaussian pulse breaks up into a series of short pulses. To further clarify the evolution of the pulse breakup process, Fig. 11 illustrates both the pulse profile and spectrum of the 100-ps input pulse. The quasi-CW input pulse from the amplifier first breaks up into a train of solitons through the MI in the fiber. In the spectrum domain, multiple sidebands can be observed with the band separation inversely proportional to the temporal separation of the soliton pulses. The generated solitons then experience frequency down-shifting due to the SSFS, with the wavelength red-shifting in the corresponding spectrum.

The SC spectrum is further broadened in the following HiNL fiber with the simulated spectrum and pulse profile shown in Fig. 12. By using a short piece of HiNL fiber, i.e., 15 cm, the spectrum is primarily broadened through SPM, combined with the contribution from other nonlinear effects, e.g., the generation of nonsolitonic dispersive wave and cross-phase modulation [4].

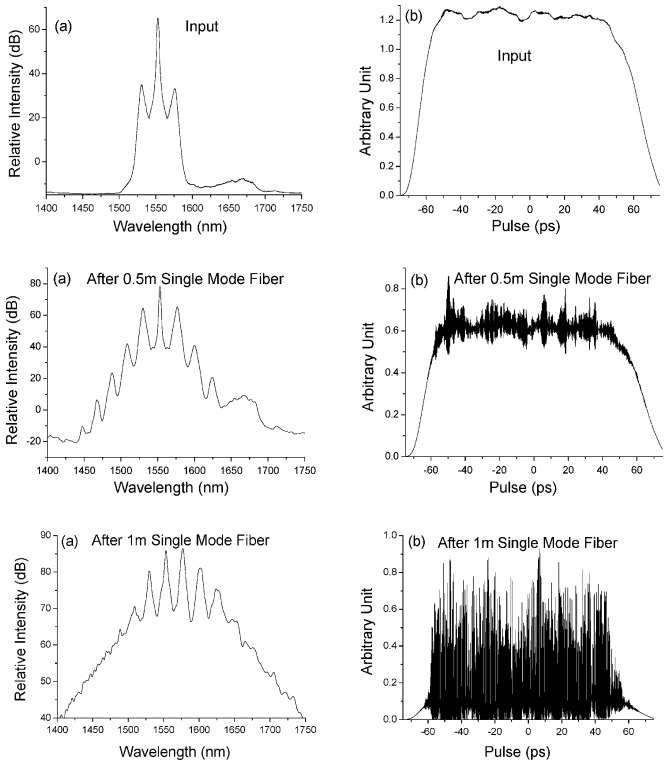

Fig. 11. (a) Spectrum and (b) pulse evolution in 1-m single-mode fiber as a function of propagation distance at 4.8-kW peak power.

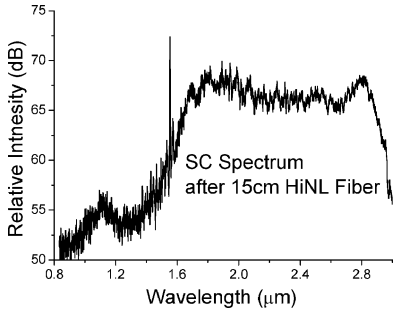

Fig. 12. Simulation result of low average power continuum after 2.75-m single-mode fiber and 15-cm HiNL fiber.

The SC spectrum is smooth and flat from ~ 1.8–$2.8\ \mu$m, whose power density is $\sim 20\,\mathrm{dB}$ higher than the short-wavelength side and is consistent with the experimental results.

Compared to the SC generation by using femtosecond laser pumping [4], we generate the SC spectrum through the ensemble average of a series of independent solitons spread in the nanosecond scale. Fig. 13 shows spectra of three subpulses sliced from the different parts of the 100-ps simulated pulse. Subpulses in the middle and trailing edge of the pulse are composed of multiple solitons and contain the entire SC spectrum. The spectrum of the subpulse from the leading edge is slightly shorter in the long-wavelength side. Because the red-shifted solitons travel slower than the blue-shifted spectral components in the anomalous dispersion environment, fewer red-shifted solitons remain in the leading edge of the pulse. Nevertheless, all the three subpulses contain most of the SC spectra with comparable spectral

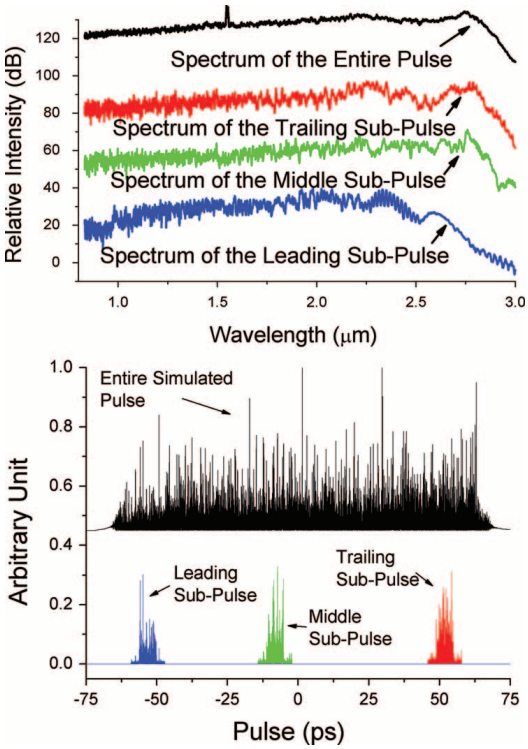

Fig. 13. Simulation results of the SC spectrum from different locations of the 100-ps pulse. The spectra of the subpulses have the similar spectral intensity and are plotted with vertical shifts for the clarification purpose.

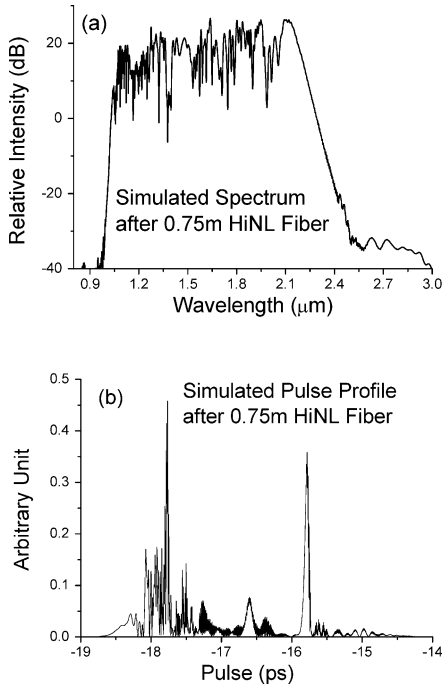

Fig. 14. Simulated SC (a) spectrum and (b) pulse profile from 1-m HiNL fiber pumped by 150-fs pulse with 15-kW peak power.

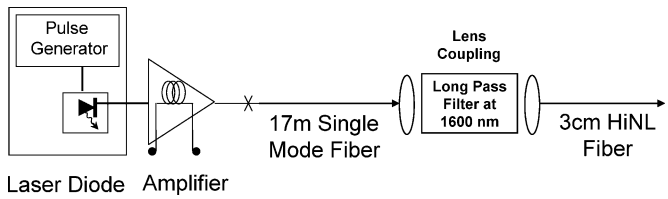

Fig. 15. Proposed experimental setup for the single-soliton SC generation.

power intensity. Therefore, the entire spectrum is a superposition of the spectra from these subpulses. Although each soliton may have a different nonlinear wavelength shift, the ensemble average of these solitons gives rise to a stable and smooth SC spectrum.

To further confirm our hypothesis, Fig. 14 simulates the SC spectrum and the corresponding pulse profile generated in 1-m length of HiNL fiber by using a femtosecond laser with pulse width of ~ 150 fs at 15-kW peak power. The femtosecond pulse breaks up into multiple solitons and dispersive waves in the time domain [4] and generates SC spectrum similar to that obtained by using nanosecond pulses. Hence, by using MI to break up the nanosecond pulses into femtosecond soliton trains, LD pulses can be used to generate SC in a similar way as femtosecond lasers. Furthermore, compared to the relatively high fluctuation and instability associated with the SC spectrum generated by using femtosecond pump laser [17], we estimate the amplitude fluctuation over the entire spectrum from pulse to pulse to be less than 1% in our system.

IV. SC Generation in Single Soliton Pulse

Simulations are carried out to concentrate the majority of the SC energy into a single pulse under nanosecond pulse pumping. As we have analyzed earlier, the SC spectrum generated by amplified nanosecond pulses results from the ensemble average of a series of solitons spread in the nanosecond scale. Therefore, the entire SC spectrum is not generated in a single short pulse, which limits its potential applications such as ultrafast time-resolved spectroscopy.

By tailoring the shape of the amplified LD pulses, we can generate a single soliton out of the entire pulse in our simulations. The proposed setup is illustrated in Fig. 15, with Fig. 16 showing the simulated temporal and spectral evolution of the pulse in the single-mode fiber. The input pulse has a rising time of ~ 10 ps and a falling time of ~ 25 ps with a peak power of ~ 500 W. By coupling the pulse into the single-mode fiber, MI phase-matches and breaks up the pulse into solitons. The pulse breakup starts in the vicinity of the pulse peak because it has the highest intensity. As the pulse continues to propagate through the fiber, more solitons are generated, which are predominantly in the trailing side of the pulse due to the asymmetric pulse shape. As the solitons compress further, the one with the highest peak power undergoes frequency down-shifting by SSFS, and moves toward the trailing edge of the pulse because of the anomalous dispersion. When the dominant soliton catches up with the rest of the solitons in the trailing side of the pump, the solitons collide with each other, and the red-shifted components in the dominant soliton are amplified by the Raman effect [11]. Therefore, the collision process contributes to a single soliton with narrow pulse width and high peak power. We can also observe a spectral peak around 1650 nm, which is red-shifted

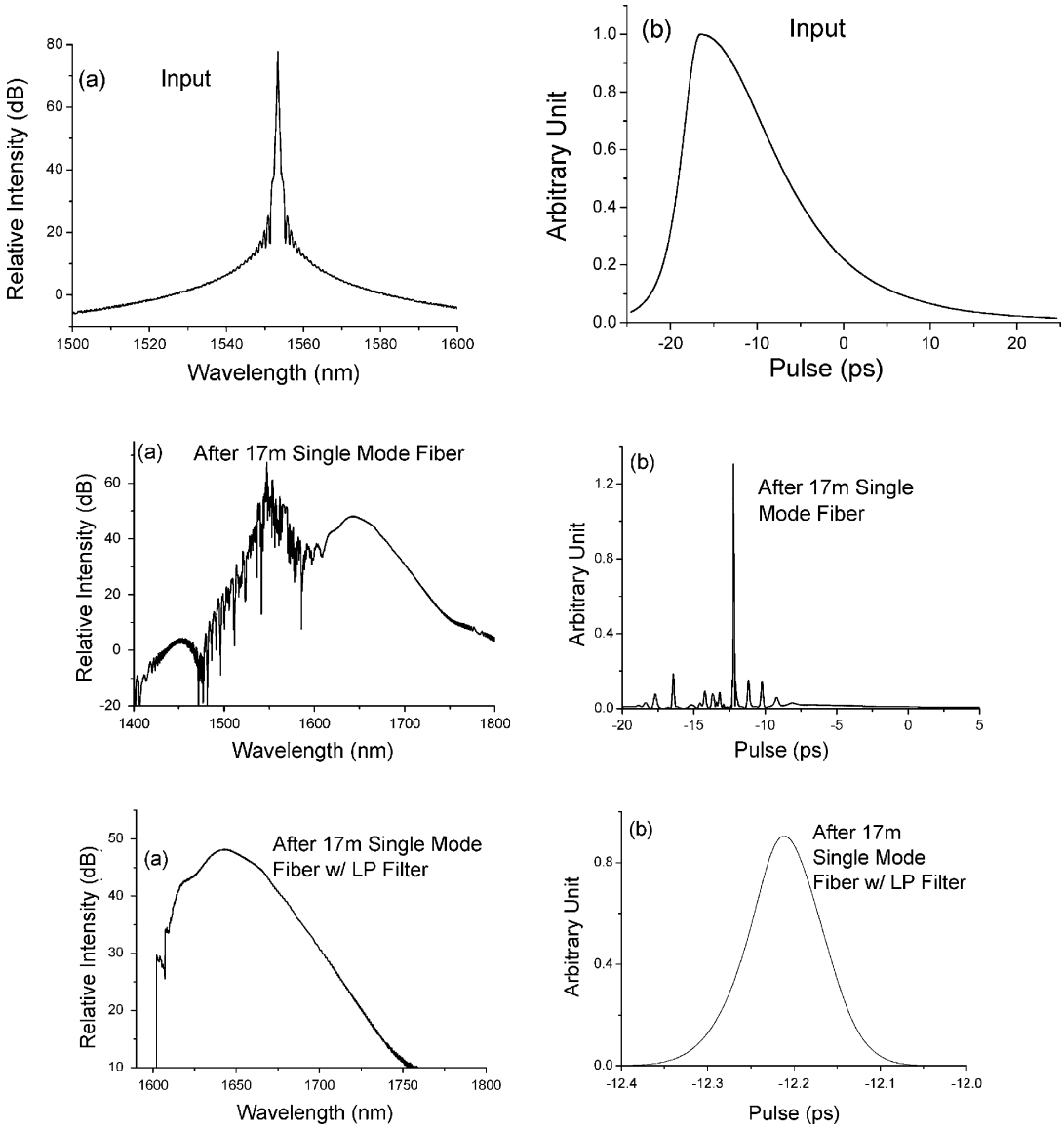

Fig. 16. (a) Spectrum (b) pulse evolution in single-mode fiber as a function of propagation distance.

by $\sim 100\,\mathrm{nm}$ from the pump due to the SSFS. By putting a 1600-nm-long pass filter to filter out the residual spectrum near the pumps, we confirm that the entire red-shift spectral peak is generated in a single dominant soliton with the pulse width of ~ 100 fs (full-width at half-maximum).

The generated single soliton is then launched into a short piece of HiNL fiber to generate a smooth SC. For example, SC with a continuous spectrum ranging over $\sim 500\,\mathrm{nm}$ can be generated in a 3-cm length of HiNL with an effective nonlinearity $\sim 9.6\,\mathrm{W}^{-1}\mathrm{km}^{-1}$ and a zero-dispersion wavelength of 1544 nm. The spectrum is broadened in the HiNL fiber primarily through SPM nonlinearity. As shown in Fig. 17, the soliton remains compressed with the pulse envelop distorted due to the contribution of self-steepening, which will eventually break up the pulse due to the group velocity difference. Therefore, without using a femtosecond laser pulse [4], we confine the entire SC spectrum in a single soliton pulse from an amplified quasi-CW pulse.

It should be noted that the pulse width of input pulse does not need to be exactly as that used in the aforementioned case. For example, we obtain a similar result by using an input pulse with ~ 15-ps rising time and ~ 50-ps falling time with ~ 400-Wpeak power. In practice, such pulse can be generated through a well-designed driving circuit or with the help of a high-bandwidth modulator.

V. Summary

We use nanosecond LD pulses amplified by multistage fiber amplifiers to generate SC from 0.8–3 μm in less than 4 m of fused silica fiber. A two-step model based on pulse breakup in single-mode fiber followed by spectral broadening in HiNL fiber is used to optimize the SC generation process, and the average power in the continuum is scaled up to 5.3 W by increasing the pulse repetition rate. We attribute the generated SC spectrum to the ensemble average of multiple solitons and

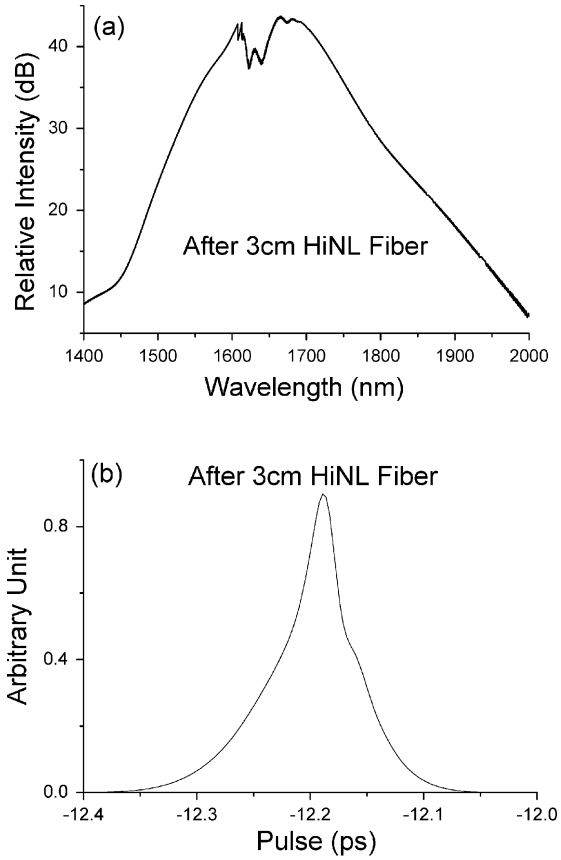

Fig. 17. (a) Spectrum (b) pulse after 17-m single-mode fiber followed by 3-cm HiNL fiber.

nonsolitonic dispersive waves. SC spectra generated through amplified nanosecond pulses are shown to be similar to the continuum generated by using femtosecond lasers. We also present a new method to generate the entire SC spectrum in a single soliton pulse by tailoring the input pulse shape.

REFERENCES

[1] R. R. Alfano, *The Supercontinuum Laser Source: Fundamentals With Updated References*, 2nd ed. New York: Springer-Verlag, 2006.

[2] J. W. Nicholson, A. D. Yablon, P. S. Westbrook, K. S. Feder, and M. F. Yan, "High power, single mode, all-fiber source of femtosecond pulses at 1550 nm and its use in supercontinuum generation," *Opt. Exp.*, vol. 12, pp. 3025–3034, 2004.

[3] A. K. Abeeluck and C. Headley, "Continuous-wave pumping in the anomalous- and normal-dispersion regimes of nonlinear fibers for supercontinuum generation," *Opt. Lett.*, vol. 30, pp. 61–63, 2005.

[4] T. Hori, N. Nishizawa, T. Goto, and M. Yoshida, "Experimental and numerical analysis of widely broadened supercontinuum generation in highly nonlinear dispersion-shifted fiber with a femtosecond pulse," *J. Opt. Soc. Amer. B*, vol. 21, pp. 1969–1980, 2004.

[5] S. Kobtsev and S. Smirnov, "Modelling of high-power supercontinuum generation in highly nonlinear, dispersion shifted fibers at CW pump," *Opt. Exp.*, vol. 13, pp. 6912–6918, 2005.

[6] G. P. Agrawal, *Nonlinear Fiber Optics*, 3rd ed. San Diego, CA: Academic, 2001.

[7] S. Moon and D. Y. Kim, "Generation of octave-spanning supercontinuum with 1550-nm amplified diode-laser pulses and a dispersion-shifted fiber," *Opt. Exp.*, vol. 14, pp. 270–278, 2006.

[8] H. Lim, Y. Jiang, Y. Wang, Y. Huang, Z. Chen, and F. Wise, "Ultrahigh-resolution optical coherence tomography with a fiber laser source at 1 μm," *Opt. Lett.*, vol. 30, pp. 1171–1173, 2005.

[9] J. N. Kutz, C. Lyngå, and B. Eggleton, "Enhanced supercontinuum generation through dispersion-management," *Opt. Exp.*, vol. 13, pp. 3989–3998, 2005.

[10] C. Xia, M. Kumar, O. P. Kulkarni, M. N. Islam, F. L. Terry, Jr., M. J. Freeman, M. Poulain, and G. Mazé, "Mid-infrared supercontinuum generation to 4.5 μm in ZBLAN fluoride fibers by nanosecond diode pumping," *Opt. Lett.*, vol. 31, pp. 2553–2555, 2006.

[11] M. N. Islam, G. Sucha, I. Bar-Joseph, M. Wegener, J. P. Gordon, and D. S. Chemla, "Femtosecond distributed soliton spectrum in fibers," *J. Opt. Soc. Amer. B*, vol. 6, pp. 1149–1158, 1989.

[12] C. Xia, M. Kumar, O. P. Kulkarni, M. N. Islam, F. L. Terry Jr., D. A. Nolan, and W. A. Wood, presented at Conf. Lasers Electro-Optics CLEO 2006, Long Beach, CA., May 21–26, 2006, Invited Talk, Paper CThV5.

[13] M. N. Islam, G. Sucha, I. Bar-Joseph, M. Wegener, J. P. Gordon, and D. S. Chemla, "Broad bandwidths from frequency-shifting solitons in fibers," *Opt. Lett.*, vol. 14, pp. 370–372, 1989.

[14] C. Xia, M. Kumar, M.-Y. Cheng, R. S. Hegde, M. N. Islam, A. Galvanauskas, H. G. Winful, F. L. Terry, Jr., M. J. Freeman, M. Poulain, and G. Mazé, "Power scalable mid-infrared supercontinuum generation in ZBLAN fluoride fibers with up to 1.3 watts time-averaged power," *Opt. Exp.*, vol. 15, pp. 865–871, 2007.

[15] T. Izawa, N. Shibata, and A. Takeda, "Optical attenuation in pure and doped fused silica in their wavelength region," *App. Phys. Lett.*, vol. 31, pp. 33–35, 1977.

[16] T. Hohage and F. Schmidt. (2002). On the numerical solution of nonlinear Schrödinger equations in fiber optics, ZIB-Rep. 02-04. [Online]. Available: ftp://ftp.zib.de/pub/zib-publications/reports/ZR-02-04.pdf

[17] K. L. Corwin, N. R. Newbury, J. M. Dudley, S. Coen, S. A. Diddams, B. R. Washburn, K. Weber, and R. S. Windeler, "Fundamental amplitude noise limitations to supercontinuum spectra generated in a microstructured fiber," *Appl. Phys. B*, vol. 77, pp. 269–277, 2003.

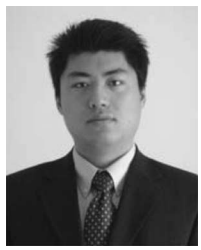

Chenan Xia received the B.S. degree in physics from Fudan University, Shanghai, China, in 2004, and the M.S. degree in electrical engineering from the University of Michigan, Ann Arbor, in 2006, where he is currently working toward the Ph.D. degree.

His current research interests include fiber-based midinfrared supercontinuum light source and its applications on spectral fingerprinting, chemical sensing, and fiber-to-the-home passive optical network.

Malay Kumar received the B.S. degree in physics from Delhi University, Delhi, India, in 2002, and M.S. degree in physics from the Indian Institute of Technology, Delhi, India, in 2004. He is currently working toward the Ph.D. degree in electrical engineering at the University of Michigan, Ann Arbor.

His research interests include high-sensitivity absorption spectroscopy using supercontinuum sources and optical metrology for imaging of automobile parts.

Ming-Yuan Cheng received the B.S. degree in electrical engineering from National Taiwan University, Taipei, Taiwan, R.O.C., in 2001, and the M.S. degree in electrical engineering from the University of Michigan, Ann Arbor, in 2003, where she is currently working toward the Ph.D. degree.

Her current research interests include high-power pulsed fiber amplifiers and fiber-based chirped pulse amplification systems.

Ojas P. Kulkarni received the B.E. degree in electronics and telecommunications from the Mumbai University, Mumbai, India, in 2004, and the M.S. degree in electrical engineering from the University of Michigan, Ann Arbor, in 2005, where he is currently working toward the Ph.D. degree.

His current research interests include modulators and supercontinuum-based sources for next-generation fiber-to-the-home passive optical network.

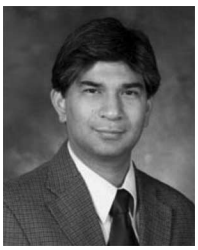

Mohammed N. Islam (M'94–SM'96–F'05) received the B.S., M.S., and Sc.D. degrees in electrical engineering from Massachusetts Institute of Technology, Cambridge, in 1981, 1983, and 1985, respectively.

From 1985 to 1992, he was a Technical Staff Member in the Advanced Photonics Department, AT&T Bell Laboratories, Holmdel, NJ. He joined the Electrical Engineering and Computer Science (EECS) Department, University of Michigan, Ann Arbor, in 1992, where he is currently a Full Tenured Professor and the Director of Undergraduate Programs. He is author or coauthor of over 112 papers published in refereed journals. He holds over 120 patents, some of which are pending. He has authored three books and has written several book chapters. His current research interests include midinfrared laser sources and their applications in fiber-to-the-home, advanced semiconductor process control, combustion monitoring, infrared countermeasures, chemical sensing, biomedical-selective laser ablation, ultrahigh resolution imaging of automobile parts such as transmissions, and modulators and new architectures for fiber-to-the-home systems. He is involved in the fields of photonics, fiber-optic communications, high-tech entrepreneurship, and patent fundamentals for engineers. He is the Founder of several spin-off companies from the University of Michigan, including Xtera Communications, Omni Sciences, Celeste Optics, AccuPhotonics, and Cheetah Omni. He is a Registered Patent Agent with the U.S. Patent and Trademark Office. He is also the Chief Technology Officer (CTO) of optics at Coherix, Inc., Ann Arbor, MI.

Prof. Islam was a Fannie and John Hertz Fellow from 1981 to 1985. In 1992, he was awarded the Optical Society of America (OSA) Adolf Lomb Medal for the pioneering contributions to nonlinear optical phenomena and all-optical switching in optical fibers. He also received the University of Michigan (UM) Research Excellence Award in 1997. He became a Fellow of the OSA in 1998. In 2002, he received the Texas eComm Ten Award for being one of the ten most influential people in Texas's digital economy. He is also the first recipient of the prestigious 2007 Distinguished University Innovator Award for developing and commercializing breakthrough technology as well as for bringing lessons learned back into the classroom through the teaching of entrepreneurship and intellectual property protection. He has also been an invited speaker at over 60 conferences and symposiums, and he has served on numerous Conference Technical Committees, Advisory Committees, and Board of Directors.

Almantas Galvanauskas was born in Vilnius, Lithuania, in 1963. He received the diploma in physics from Vilnius University, Vilnius, Lithuania, in 1986, and the Ph.D. degree in physics from the Royal Institute of Technology, Stockholm, Sweden, in 1992.

From 1993 to 2001, he was with IMRA America Inc., Ann Arbor, MI, where he was engaged in research and development of high-energy and high-power femtosecond fiber laser technology. Since 2002, he has been an Associate Professor in the Electrical Engineering and Computer Science Department, University of Michigan, Ann Arbor. His current research interests include nonlinear optics, fiber optics, ultrashort pulse, and high-intensity fiber lasers and their use for a variety of laser plasma applications.

Dr. Galvanauskas is a member of the Optical Society of America.

Fred L. Terry, Jr., (S'78–M'80–SM'99), photograph and biography not available at the time of publication.

Mike J. Freeman, photograph and biography not available at the time of publication.

Daniel A. Nolan (M'88) received the Ph.D. degree in physics from the Pennsylvania State University, University Park, in 1974.

His research was concerned with the field of surface physics, in particular, the adsorption of particles on metallic surfaces. He joined the Corning, Inc., Corning, NY, in 1974, where he is currently a Corning Fellow in the Research Directorate. He investigated the formation of color centers and the photokinetic processes in photochromic and polarizing glasses. This research contributed to the introduction of Corning's Polarcor polarizing glass. His current research interests include optical fiber, optical materials, propagation of light in both single-mode and multimode fibers, polarization optics, nonlinear effects in fibers, fiber-optic sensors, and planar- and fiber-based passive components for local area networks. He made contributions to the understanding of light propagation in multimode and single-mode fibers. He initiated the optical propagation research meetings, which provided an important forum and background for the invention LEAF. He also provided theories and models important for the introduction of multimode fibers including codes 1509 and 1517. He initiated a polarization mode dispersion research program, which has led to a number of process implementations at Wilmington. From 1984 to 1992, he was responsible for Corning Research activities in fiber-based passive components, investigation and development of a number of important components including splitters, taps, switches, variable optical attenuators (VOAs), $1 \times n$ devices, amplifier components, and the introduction of MultiClad coupler. These devices are used throughout the world and almost exclusively in all undersea fiber-optic amplified systems. The VOAs and wavelength division multiplexers (WDMs) continue to be manufactured at Avanex. He has coauthored five books on the subject of optical fiber and optical components. His book *WDM Components* published in 1999 is a best seller for the Optical Society of America. He holds 58 U.S. patents.

Dr. Nolan is a Fellow of the Optical Society of America. He has presented invited papers on passive components at the Optical Fiber Conference (OFC) from 1991 to 1993. He has taught a course on passive components at OFC in 1993 and 1994. He has been a member of committees for important fiber-optic-related conferences such as the OFC (1991–1993), Integrated Photonics Research (IPR) (1992–1994), Conference on Lasers and Electro-Optics (CLEO) (1989–1990, 2000–2003), and European Conference on Optical Communications (ECOC) (2000–2005). During 1990–1995, he was an Associate Editor of the IEEE PHOTONIC TECHNOLOGY LETTERS. During 1991–1993, he was an Associate Editor of *Fiber and Integrated Optics*. He is a member of the Steering Committee for the OSA/IEEE JOURNAL OF LIGHTWAVE TECHNOLOGY. He has published many articles on fibers and on integrated optics in the OSA/IEEE JOURNAL OF LIGHTWAVE TECHNOLOGY and other important IEEE and OSA publications including *Optics Letters*. He has published a number of papers on photochromic and polarizing glass in the *Journal of Solids*, *Journal of the Optical Society of America*, *Journal of the American Ceramic Society*, and *Physics Review*. He is also a Fellow of the Optical Society of America. He received the Penn State Outstanding Alumni Award from the College of Science for his contributions to optical communications. He received Corning's Outstanding Publication Award in 1989 and Prestigious Stookey for Exploratory Research in 1995. He received an IR100 Award for the invention of infrared polarizing glass Polarcor.

William A. Wood received the Ph.D. degree in mathematical physics from Indiana University, Bloomington, in 1991.

He was a Visiting Assistant Professor of physics at Indiana University and the University of Louisville, Louisville, KY. He was a Radar Systems Engineer in Technology Service Corporation. From 1999 to 2005, he was a Staff Scientist with Corning, Inc., Corning, NY, where he specialized in rare-earth doped and dispersion compensating fiber development, and later moved to a research group. He holds ten U.S. patents. He is the author or coauthor of several publications.

Dr. Wood is a member of the American Physical Society, the American Mathematical Society, and the Society for Information Display.